

Stability conditions in the Thomas-Fermi approximation and small amplitude vibrations in the Vlasov equation

S. J. Lee, E. D. Cooper, H. H. Gan, and S. Das Gupta
Physics Department, McGill University, Montreal, P.Q., Canada H3A 2T8
 (Received 12 June 1989)

We derive a stability condition for the Thomas-Fermi solution of a finite nucleus where the underlying force has a finite range. The stability condition can be cast in the form of an eigenvalue equation; these eigenvalues must be all positive. The lowest eigenmodes correspond closely to vibration modes. The relationship of this time-independent formulation to the time-dependent Vlasov equation with self-consistent potential is established.

I. INTRODUCTION

Time-dependent Hartree-Fock approximation (TDHF) has been used extensively in the past to analyze heavy-ion collisions at low to moderate energies. Here the single nucleon orbitals ψ_i evolve according to

$$(T + U)\psi_i = i\hbar \frac{\partial \psi_i}{\partial t} . \quad (1)$$

In the static Hartree-Fock case, $(T + U)\psi_i = \epsilon_i \psi_i$ and the time dependence of ψ_i is trivial. The time-dependent Vlasov equation can be derived as a semiclassical approximation to TDHF. Define a phase space density $f(\mathbf{r}, \mathbf{p}, t)$ using the Wigner transform

$$f(\mathbf{r}, \mathbf{p}, t) = \frac{1}{(2\pi\hbar)^3} \int d^3s e^{-i\mathbf{p}\cdot\mathbf{s}/\hbar} \times \sum_i \psi_i^* \left[\mathbf{r} - \frac{\mathbf{s}}{2}, t \right] \times \psi_i \left[\mathbf{r} + \frac{\mathbf{s}}{2}, t \right] , \quad (2)$$

then, with some approximations,^{1,2} the following rule for the time evolution of $f(\mathbf{r}, \mathbf{p}, t)$ follows from Eq. (1):

$$\frac{\partial}{\partial t} f(\mathbf{r}, \mathbf{p}, t) + \frac{\mathbf{p}}{m} \cdot \nabla f(\mathbf{r}, \mathbf{p}, t) - [\nabla U(\mathbf{r}, t)] \cdot \nabla_p f(\mathbf{r}, \mathbf{p}, t) = 0 , \quad (3)$$

where ∇ and ∇_p mean the gradients in r and p space, respectively. Numerical calculations³ show that Eq. (3) does reproduce great similarities with the bulk dynamics predicted by Eq. (1).

There is another reason the Vlasov prescription has become so relevant in nuclear physics in recent times. Approximation schemes have been devised which allow one to solve transport equations beyond the collisionless limit, i.e., when the right-hand side of Eq. (3) is replaced by the Boltzmann-Uehling-Uhlenbeck collision integral (BUU). Extensive calculations have been made which compare theoretical results with experimental data. Details can be found in Ref. 1.

To study peripheral heavy-ion collisions using BUU, it is necessary to construct static Vlasov solutions with diffuse surfaces as pointed out in Ref. 4. To produce a reasonable surface in a semiclassical limit, one needs to introduce a finite range force such as a Yukawa interaction⁵ or a gradient-dependent interaction.⁶ Properties of self-consistent solutions in the Thomas-Fermi approximation using a finite range force are discussed in Refs. 7 and 8. The purpose of the present paper is to investigate the stability of the self-consistent solutions in this semiclassical approximation. In quantum calculations, stability condition of a static Hartree-Fock solution requires that the eigenvalues of the random-phase-approximation (RPA) matrix be all real. This feature of quantum calculations has been known for more than 25 years;^{9,10} curiously enough, the stability conditions of the semiclassical approximation seem not to have been formulated before although the approximation has been known almost since the advent of quantum mechanics.^{11,12}

With a finite range force, the analogy of the semiclassical Vlasov description with Hartree-Fock (quantum) becomes more revealing. A similar stability matrix can be derived for the Vlasov solution; for the self-consistent Vlasov solution to be stable, the eigenvalues of this matrix must all be positive. What is quite striking is that, for the spherically symmetric nucleus, the solutions with the lowest eigenvalues very much resemble what one intuitively expects to be the characteristics of multipole modes of vibration; for example, the transition density $\delta\rho$ for a breathing mode is proportional to the difference between the self-consistent density and a scaled self-consistent density which has the same number of nucleons:

$$\delta\rho(r) = [\alpha^3 \rho(\alpha r) - \rho(r)]_{\alpha=1+\delta\alpha} \approx \left[3\rho(r) + r \frac{\partial}{\partial r} \rho(r) \right] \delta\alpha , \quad (4)$$

where $\delta\alpha$ is an infinitesimal constant.² We can also relate these time-independent considerations to a time-dependent picture where a small departure from the self-consistent solution leads to a harmonic vibration. Small amplitude oscillation of a Vlasov solution has been dis-

cussed in the literature before.^{2,13-15}

The stability matrix for a static Vlasov solution with a finite range force has been derived in Ref. 5. For completeness and in order to define our notations, this will be summarized in Sec. II. The eigensolutions of this matrix will be discussed in Sec. III. In Sec. IV we will derive a dispersion relation using the time-dependent Vlasov equation with self-consistent potential. The same stability matrix appears in the dispersion relation which leads us to understand the relationship between stability and vibration modes. Finally, the conclusions will be presented in Sec. V.

II. STABILITY CONDITION

In Ref. 5 we have shown that the self-consistent solution of a static Vlasov equation produces an extremum in the total energy. To investigate the stability of the self-consistent solution, we consider a variation of energy. For the variation of energy with respect to the density, we need to express the total energy in terms of density. Consider the Wigner function $f(\mathbf{r}, \mathbf{p})$ for a static nucleus. The nucleon density in a nucleus is $\rho(\mathbf{r}) = \int d^3p f(\mathbf{r}, \mathbf{p})$. The potential energy we are considering here for the Vlasov equation of Eq. (3) depends only upon $\rho(\mathbf{r})$ and \mathbf{r} but not upon \mathbf{p} and is of the form⁵

$$V = \sum_i \frac{1}{\sigma_i + 1} C_i \int d^3r \rho^{\sigma_i + 1}(\mathbf{r}) + \frac{1}{2} \int d^3r d^3r' \rho(\mathbf{r}) v(\mathbf{r}, \mathbf{r}') \rho(\mathbf{r}'), \quad (5)$$

where $\sigma_i \geq 1$, v has the dimension of energy, and the C_i 's have dimensions of energy times $\text{fm}^{3\sigma_i}$. For the numerical calculations in this work, we will take $v(\mathbf{r}, \mathbf{r}')$ to be a Yukawa;

$$v(\mathbf{r}, \mathbf{r}') = V_y \frac{e^{-|\mathbf{r}-\mathbf{r}'|/a_y}}{|\mathbf{r}-\mathbf{r}'|/a_y} = 4\pi V_y \sum_{l,m} f_l(r, r', a_y) Y_l^m(\hat{\mathbf{r}}) Y_l^{m*}(\hat{\mathbf{r}}'), \quad (6)$$

where

$$f_l(r, r', a_y) = i_l \left[\frac{r <}{a_y} \right] k_l \left[\frac{r >}{a_y} \right],$$

and where i_l and k_l are modified spherical Bessel functions and $\hat{\mathbf{r}}$ and $\hat{\mathbf{r}}'$ represent (θ, ϕ) and (θ', ϕ') , respectively. For spherically symmetric problems, we will only need

$$i_0(x) = \frac{\sinh(x)}{x}, \quad (7)$$

$$k_0(x) = \frac{e^{-x}}{x}.$$

The arguments presented here are valid for a general $v(\mathbf{r}, \mathbf{r}')$, including $v(\mathbf{r}, \mathbf{r}') \propto \delta(\mathbf{r}-\mathbf{r}') \nabla^2$ which is a gradient-dependent interaction,⁶ although the numerical work specifically uses the Yukawa form.

The kinetic energy density is given by $T(\mathbf{r}) = \int d^3p (p^2/2m) f(\mathbf{r}, \mathbf{p})$. Since we are looking for a

minimum in energy, it makes sense to minimize the kinetic energy for a given $\rho(\mathbf{r})$, i.e., for a fixed potential energy V [Eq. (5)]. This is achieved by letting $f(\mathbf{r}, \mathbf{p})$ be nonzero from $p=0$ to some maximum $p_F(\mathbf{r})$. Furthermore, the Hartree-Fock density matrix condition $\rho^2 = \rho$ requires the Wigner function in a classical approximation to be a step function. Thus we will have the Thomas-Fermi approximation;

$$f(\mathbf{r}, \mathbf{p}) = \frac{4}{h^3} \theta(p_F(\mathbf{r}) - p), \quad (8)$$

where 4 is the spin-isospin degeneracy factor. Here, $p_F(\mathbf{r})$ is a non-negative real quantity and the local Fermi surface is spherically symmetric. For this Wigner function,

$$\rho(\mathbf{r}) = \frac{4\pi}{3} \frac{4}{h^3} p_F^3(\mathbf{r}), \quad (9)$$

$$T(\mathbf{r}) = \frac{4\pi}{5} \frac{4}{h^3} \frac{p_F^5(\mathbf{r})}{2m} = C \rho^{5/3}(\mathbf{r}), \quad (10)$$

where

$$C = \frac{3}{5} \frac{1}{2m} \left[\frac{3}{4\pi} \frac{h^3}{4} \right]^{2/3} = \frac{3h^2}{10m} \left[\frac{3}{16\pi} \right]^{2/3}. \quad (11)$$

The total energy of the system is $E = T + V$, where the potential energy V is given by Eq. (5) and the kinetic energy is, from Eq. (10),

$$T = \int d^3r T(\mathbf{r}) = C \int d^3r \rho^{5/3}(\mathbf{r}). \quad (12)$$

The number of nucleons in the nucleus is given by

$$N = \int d^3r \rho(\mathbf{r}). \quad (13)$$

Since the energy is a function of only the density, we can minimize the energy with respect to the density.

We now consider an infinitesimal variation of density from its equilibrium density, i.e., changing $\rho(\mathbf{r})$ to $\rho(\mathbf{r}) + \delta\rho(\mathbf{r})$. For particle number conservation, we require

$$\int d^3r \delta\rho(\mathbf{r}) = 0. \quad (14)$$

The total energy can be expanded in terms of $\delta\rho(\mathbf{r})$ as, up to second order,

$$E = E_0 + \int d^3r h(\mathbf{r}) \delta\rho(\mathbf{r}) + \frac{1}{2} \int d^3r d^3r' \delta\rho(\mathbf{r}) S(\mathbf{r}, \mathbf{r}') \delta\rho(\mathbf{r}'), \quad (15)$$

where E_0 is evaluated with equilibrium density $\rho(\mathbf{r})$ and the mean-field Hamiltonian $h(\mathbf{r})$ and the stability matrix $S(\mathbf{r}, \mathbf{r}')$ are

$$h(\mathbf{r}) = \frac{\delta E}{\delta\rho(\mathbf{r})} = \frac{5}{3} C \rho^{2/3}(\mathbf{r}) + \sum_i C_i \rho^{\sigma_i}(\mathbf{r}) + \int d^3r' v(\mathbf{r}, \mathbf{r}') \rho(\mathbf{r}'), \quad (16)$$

$$\begin{aligned}
S(\mathbf{r}, \mathbf{r}') &= \frac{\delta^2 E}{\delta\rho(\mathbf{r})\delta\rho(\mathbf{r}')} \\
&= \frac{\delta h(\mathbf{r})}{\delta\rho(\mathbf{r}')} \\
&= \left[\frac{10}{9} C \rho^{-1/3}(\mathbf{r}) + \sum_i C_i \sigma_i \rho^{\sigma_i - 1}(\mathbf{r}) \right] \\
&\quad \times \delta(\mathbf{r} - \mathbf{r}') + v(\mathbf{r}, \mathbf{r}'). \quad (17)
\end{aligned}$$

Expansion of the nucleon number is

$$N = N_o + \int d^3r \delta\rho(\mathbf{r}), \quad (18)$$

where N_o is the same as Eq. (13) with the equilibrium density. Notice that, in Eq. (18), there are no higher-order terms and the second term is zero if we consider the condition of Eq. (14) explicitly.

To minimize the energy with a constraint of particle number conservation, we consider the expansion of $E - \lambda N$ in terms of $\delta\rho$ as, from Eqs. (15) and (18) up to second order,

$$\begin{aligned}
E - \lambda N &= (E_o - \lambda N_o) + \int d^3r [h(\mathbf{r}) - \lambda] \delta\rho(\mathbf{r}) \\
&\quad + \frac{1}{2} \int d^3r d^3r' \delta\rho(\mathbf{r}) S(\mathbf{r}, \mathbf{r}') \delta\rho(\mathbf{r}'), \quad (19)
\end{aligned}$$

where λ is a Lagrange multiplier for the first-order variation. For the equilibrium density, we require that the first-order term in the above equation be zero for arbitrary $\delta\rho$. Thus we have the equilibrium equation as

$$h(\mathbf{r}) - \lambda = \frac{1}{2m} \left[\frac{3}{4\pi} \frac{h^3}{4} \right]^{2/3} \rho^{2/3}(\mathbf{r}) + U(\mathbf{r}) - \lambda = 0, \quad (20)$$

where Eq. (11) has been used for C and the mean-field potential U is

$$U(\mathbf{r}) = \frac{\delta V}{\delta\rho(\mathbf{r})} = \sum_i C_i \rho^{\sigma_i}(\mathbf{r}) + \int d^3r' v(\mathbf{r}, \mathbf{r}') \rho(\mathbf{r}'). \quad (21)$$

Using Eq. (9) and remembering that $p_F(\mathbf{r})$ is real non-negative, Eq. (20) can be rewritten by

$$\frac{1}{2m} p_F^2(\mathbf{r}) = [\lambda - U(\mathbf{r})] \theta(\lambda - U(\mathbf{r})), \quad (22)$$

which is the Thomas-Fermi approximation. This is the same as the self-consistent equation for a static Vlasov solution [see Eqs. (17) and the one above it in Ref. 5]. Thus finding a self-consistent solution is equivalent to finding an extremum in energy. Due to the theta function in Eq. (22), there is a nuclear surface outside of which the self-consistent density becomes exactly zero. In Ref. 5, we have discussed extensively how to solve Eq. (22) numerically and what force parameter values give reasonable nuclear surfaces with a finite range Yukawa force in this semiclassical approximation.

For the stability of the self-consistent solution, the second order term in Eq. (19) should be positive, i.e.,

$$\int d^3r d^3r' \delta\rho(\mathbf{r}) S(\mathbf{r}, \mathbf{r}') \delta\rho(\mathbf{r}') > 0. \quad (23)$$

This will be satisfied if, in the following eigenvalue equation

$$\int d^3r' S(\mathbf{r}, \mathbf{r}') g(\mathbf{r}') = \epsilon g(\mathbf{r}), \quad (24)$$

the eigenvalue ϵ is always greater than zero. Here, for the second-order variation, $g(\mathbf{r})$ must satisfy explicitly, due to Eq. (14),

$$\int d^3r g(\mathbf{r}) = 0, \quad (25)$$

and we choose the normalization condition according to

$$\int d^3r [g(\mathbf{r})]^2 = 1 \text{ fm}^{-3}. \quad (26)$$

Equation (24) is the same as Eq. (28) in Ref. 5 except the factor of $\frac{1}{2}$ convention. It is nontrivial to solve Eq. (24) with the constraint of Eq. (25). Since $S(\mathbf{r}, \mathbf{r}')$ of Eq. (17) is symmetric in \mathbf{r} and \mathbf{r}' for the case of $v(\mathbf{r}, \mathbf{r}') = v(|\mathbf{r} - \mathbf{r}'|)$, the eigenvalues ϵ are all real. Furthermore, since $S(\mathbf{r}, \mathbf{r}')$ is infinity when $\rho(\mathbf{r}) = 0$ due to the first term of Eq. (17), the eigenvalue equation (24) tells us that $g(\mathbf{r})$ must be zero outside of the nucleus.

The total energy of the system with a small deviation of $\delta\rho(\mathbf{r}) \propto g(\mathbf{r})$ becomes

$$E = E_o + \frac{1}{2} \epsilon \int d^3r [\delta\rho(\mathbf{r})]^2. \quad (27)$$

The first term is the ground-state energy of a nucleus with self-consistent density and the second term is the excitation energy due to this density variation. Notice that the excitation energy depends on the eigenvalue ϵ and on the amplitude of $\delta\rho$ and that the eigenvalue ϵ has the dimension of energy times fm^3 . The discussions in this section are general for a momentum independent potential energy given by Eq. (5) except that we have assumed the Wigner function to be of the form of Eq. (8) (Thomas-Fermi approximation). This constraint led us to have Eq. (12), which is a simple expression of the kinetic energy in terms of the density. If Eq. (12) is satisfied within a reasonable approximation, the discussions in this section are true even for a more general Wigner function than Eq. (8) such as some we will consider later for a time-dependent Vlasov equation.

The numerical solution of Eq. (24) will be discussed in the next section. This has the constraint of Eq. (25), hence we have also considered variations in terms of other variables which are related to $\rho(\mathbf{r})$. One such variable is $z(\mathbf{r})$ where we define $z(\mathbf{r})$ through

$$\rho(\mathbf{r}) = N \frac{z^2(\mathbf{r})}{\int d^3r' z^2(\mathbf{r}')}. \quad (28)$$

The advantage of such a formulation is that number conservation is automatically satisfied when we change $z(\mathbf{r})$ to $z(\mathbf{r}) + \delta z(\mathbf{r})$. However, the stability matrix $S(\mathbf{r}, \mathbf{r}')$ is now much more complicated and no significantly new features are obtained by considering this alternative variation.

III. NUMERICAL SOLUTION OF STABILITY EQUATION

In the preceding section, we have changed the stability condition for the self-consistent solution of a static Vlasov equation into an eigenvalue problem, Eq. (24), of a stability matrix $S(\mathbf{r}, \mathbf{r}')$. Since the stability matrix $S(\mathbf{r}, \mathbf{r}')$

of Eq. (17) is symmetric in \mathbf{r} and \mathbf{r}' , the eigenfunctions $g(\mathbf{r})$ are orthogonal to each other. Thus it is reasonable to use a multipole expansion of $g(\mathbf{r})$ for a finite nucleus:

$$g(\mathbf{r}) = \sum_{l,m} g_l^m(r) Y_l^m(\hat{r}), \quad (29)$$

where $g_l^m(r)$ can be found from the eigenvalue equation. As we discussed after Eq. (26) in the preceding section, $g_l^m(r)$ must be zero outside of a nucleus due to the first term of Eq. (17). With this expansion, the nonlocal term in Eq. (17) of $S(\mathbf{r}, \mathbf{r}')$ contributes to Eq. (24) as

$$\int d^3r' v(\mathbf{r}, \mathbf{r}') g_l^m(r') Y_l^m(\hat{r}') \\ = 4\pi V_y \left[\int dr' r'^2 f_l(r, r', a_y) g_l^m(r') \right] Y_l^m(\hat{r}) \quad (30)$$

for a Yukawa force given by Eq. (6) due to the orthonormality of the spherical harmonics $Y_l^m(\hat{r})$. Thus the Yukawa force does not couple a multipole component of Eq. (29) to any other component. For a nucleus which is spherically symmetric in its ground state, each component of the expansion Eq. (29) becomes an eigenfunction of Eq. (24). Furthermore, since $f_l(r, r', a_y)$ is independent of m , $g_l^m(r) Y_l^m(\hat{r})$ are degenerate for different values of m for a fixed l with $g_l^m(r) = g_l(r)$. Thus, for simplicity, we will consider only a spherically symmetric nucleus in this section. For this case, we only need to consider the $m=0$ case and can handle each multipole mode separately. The normalization condition Eq. (26) for each multipole mode becomes

$$\int d^3r [g(\mathbf{r})]^2 = \int dr r^2 [g_l(r)]^2 = 1. \quad (31)$$

For a spherical nucleus, due to the symmetry property and analyticity, the self-consistent density can be approximated to be $\rho(\mathbf{r}) \approx c_0 + c_2 r^2$ for small r where c_0 and c_2 are constants. This behavior of $\rho(\mathbf{r})$ at the $r \approx 0$ region can be shown from the self-consistent equation (20) for Yukawa force. On the other hand, the small r behavior of Eq. (30) for $f_l(r, r', a_y)$ given by Eq. (6) becomes $\approx cr^l$ since $i_l(r) \propto r^l$ for $r \approx 0$. Thus, for Eq. (24), the lowest order dependence of r in $g_l(r)$ would be r^l in the $r \approx 0$ region for a spherical nucleus. This can be shown more rigorously by changing the integral equation (24) into a differential equation using the fact that the Yukawa field is a solution of the Helmholtz equation. Equation (25) for the particle number conservation is automatically satisfied for nonzero l due to the angular dependence $Y_l^m(\hat{r})$, i.e.,

$$\int d^3r g_l(r) Y_l^m(\hat{r}) = \sqrt{4\pi} \int dr r^2 g_l(r) \delta_{l,0} \delta_{m,0}. \quad (32)$$

Therefore we need to consider the condition of Eq. (25) explicitly only for the $l=0$ case.

For the $l > 0$ case, g_l can be expanded in terms of

$$\phi_n^l(r) = \begin{cases} \mathcal{N}_n^l j_l(k_n^l r) & \text{for } r \leq R \\ 0 & \text{for } r > R, \end{cases} \\ k_n^l = r_n^l / R, \quad (33)$$

where r_n^l is the n th zero point of $j_l(r)$, i.e., $j_l(r_n^l) = 0$, \mathcal{N}_n^l is the normalization constant of $\phi_n^l(r)$ through

$\int dr r^2 [\phi_n^l(r)]^2 = 1$ due to Eq. (31), and R is the nuclear surface radius, i.e., $\rho(\mathbf{r}) = 0$ for $r \geq R$. These functions $\phi_n^l(r)$ for $l > 0$ satisfy all the conditions of $g_l(r)$ we have discussed.

For $l=0$, we require explicitly

$$\int d^3r g(\mathbf{r}) = \sqrt{4\pi} \int dr r^2 g_0(r) = 0. \quad (34)$$

Because of this constraint, we cannot use $\phi_n^0(r)$ of Eq. (33) as a basis function. Due to orthogonality of spherical Bessel functions $j_l(k_n r)$, the following functions $\phi_{mn}(r)$ for $l=0$ satisfy all the properties of $g_0(r)$ we have discussed including the constraint of Eq. (34):

$$\phi_{mn}(r) = \begin{cases} j_0(k_m r) j_0(k_n r) & \text{for } r \leq R \\ 0 & \text{for } r > R, \end{cases} \quad (35)$$

$$k_n = (n+1)\pi/R,$$

where $m \geq 0, n \geq 0$ with $m \neq n$, and R is the nuclear surface radius. These $\phi_{mn}(r)$'s with all values of m and n are over complete, that is, linearly dependent. However, $j_0(k_n r)$'s with all $n \geq 0$ form a complete set in a Hilbert space of functions which satisfy all the properties of $g_0(r)$ except the constraint of Eq. (34). Thus fixing one of m and n to be a specific value, say $m=0$, $\phi_{0n}(r)$'s with all $n \geq 1$ are linearly independent and form a complete set in a Hilbert space of functions which satisfy all the properties of $g_0(r)$ including the condition of zero volume integral Eq. (34). But these are not orthonormal. However, we can get orthonormalized functions from Eq. (35) by the Gram-Schmidt method. Let us call the orthonormalized basis functions $\phi_n(r)$, i.e.,

$$\phi_n(r) = \begin{cases} \vartheta[j_0(k_0 r) j_0(k_n r)] & \text{for } r \leq R \\ 0 & \text{for } r > R, \end{cases} \quad (36)$$

where ϑ represents Gram-Schmidt orthonormalization of the function in the square bracket, k_0 and k_n are given in Eq. (35), and $n \geq 1$.

Now, for each multipole mode with a given l , we can expand the eigenfunction $g(r)$ with an eigenvalue ϵ of Eq. (24) in terms of the basis functions $\phi_n(r)$ [Eq. (36) for monopole and Eq. (33) for others] as

$$g(r) = \sum_n a_n \phi_n(r), \quad (37)$$

with normalization condition

$$\sum_n (a_n)^2 = 1,$$

where $g(r) = g_l(r)$. Here n goes from 1 to infinity; in practice n is truncated to a high value N such that the lowest eigenfunctions would be unaffected by increasing the dimensionality. In this basis space, Eq. (24) becomes, in a matrix form,

$$\begin{pmatrix} S_{11} & S_{12} & \cdots & S_{1N} & \cdots \\ S_{21} & S_{22} & \cdots & S_{2N} & \cdots \\ \vdots & \vdots & \ddots & \vdots & \ddots \\ S_{N1} & S_{N2} & \cdots & S_{NN} & \cdots \\ \vdots & \vdots & \ddots & \vdots & \ddots \end{pmatrix} \begin{pmatrix} a_1 \\ a_2 \\ \vdots \\ a_N \\ \vdots \end{pmatrix} = \epsilon \begin{pmatrix} a_1 \\ a_2 \\ \vdots \\ a_N \\ \vdots \end{pmatrix}, \quad (38)$$

where

$$\begin{aligned}
S_{mn} &= \int d^3r d^3r' \varphi_m(r) Y_l^0(\hat{r}) S(\mathbf{r}, \mathbf{r}') \varphi_n(r') Y_l^0(\hat{r}') \\
&= \int dr r^2 \varphi_m(r) \left[\frac{10}{9} C \rho^{-1/3}(r) + \sum_i C_i \sigma_i \rho^{\sigma_i - 1}(r) \right] \varphi_n(r) + 4\pi V_y \int dr r^2 dr' r'^2 \varphi_m(r) f_l(r, r', a_y) \varphi_n(r'), \quad (39)
\end{aligned}$$

for $S(\mathbf{r}, \mathbf{r}')$ of Eq. (17). For the nonlocal term in $S(\mathbf{r}, \mathbf{r}')$, Eq. (30) has been used.

For numerical calculations in this work, we have chosen the potential energy Eq. (5) to have only one local interaction term and one Yukawa force Eq. (6) with [see Eq. (29) of Ref. 5]

$$\begin{aligned}
C_1 &= 3238.1 \text{ MeV fm}^6, \quad \sigma_1 = 2, \\
V_y &= -668.65 \text{ MeV}, \quad a_y = 0.45979 \text{ fm}. \quad (40)
\end{aligned}$$

This potential is the simplest form and gives reasonable fit to the diffuse surface and the binding energy simultaneously for a symmetric nucleus.⁵ The force parameters in Eq. (40) give the same nuclear matter properties as Bonche-Koonin-Negele (BKN) force¹⁶ and the attractive local force of BKN has been absorbed entirely into an augmented Yukawa field whose range a_y is kept unchanged from the original BKN value. In the present work, for simplicity, we have neglected the Coulomb interaction and the symmetry energy of the nuclear force. For this force, we can get the self-consistent density $\rho(r)$ of the static Vlasov equation using Eq. (20). The details of numerical calculation of this have been discussed in Ref. 5. For the matrix element Eq. (39), we have calculated the self-consistent density $\rho(r)$ in the radial grid space of $\Delta r = 0.0125$ fm.

The lowest three eigenvalues for $l=0$ to 4 for ^{16}O , ^{40}Ca , and ^{208}Pb are given in Table I. For $l=1$, the calculated lowest eigenvalues are ≈ 0.2 MeV in magnitude; this reflects numerical inaccuracy originating from the finite grid size, the truncated basis space, and the numerical value of the nuclear radius R ; the exact eigenvalue is

zero and is related to the translational movement of the self-consistent Vlasov density. The rest of the eigenvalues are truly positive definite. We work with a basis space of $N=100$ and the lowest several eigenvalues change by less than 1 MeV fm³ when we go from $N=50$ to 100 and when we go from $\Delta r=0.0125$ to 0.025 fm. Some of the normalized eigenvectors $g(r)$ [Eq. (37)] of the stability matrix are shown in Fig. 1 for ^{40}Ca . The small ripples at small r region in this figure are due to the numerical problems and reflect the fact that plane waves are all degenerate eigensolutions of stability matrix in the nuclear matter limit. The lowest $l=0$ excitation mode has one node and the lowest $l>0$ modes have no node (solid line in Fig. 1). The eigenvalues increase with l for the same number of nodes and become smaller for larger nuclei. Similar dependences on l and on the nuclear size of the eigenvalues for modes with zero node have been seen in the resonance energy of the isoscalar multipole vibration modes (see Fig. 5 in Ref. 17).

What is very striking is the similarity in the eigenfunctions of our stability matrix and the multipole vibration modes. For an inhomogeneous nuclear fluid, the transition density from its equilibrium density $\rho(\mathbf{r})$ satisfies the continuity equation,

$$\frac{\partial}{\partial t} \delta\rho(\mathbf{r}, t) = -\nabla \cdot [\rho(\mathbf{r}) \mathbf{u}(\mathbf{r}, t)], \quad (41)$$

where \mathbf{u} is the local average velocity. With irrotational ($\nabla \times \mathbf{u} = 0$) and incompressibility ($\nabla \cdot \mathbf{u} = 0$) assumption, Eq. (41) determines the multipole expansion of the vibrational transition density. For a spherical nucleus,

TABLE I. Eigenvalues ϵ of the stability matrix Eq. (24) for the multipole modes of $0 \leq l \leq 4$ in MeV fm³. There is no zero node mode for the monopole ($l=0$) case.

No. of nodes	$l=0$	1	2	3	4
^{16}O					
0		0.17	37.14	78.80	120.19
1	239.63	294.47	325.10	349.79	368.80
2	372.65	407.80	418.98	424.85	428.12
3	429.18				
^{40}Ca					
0		-0.11	22.54	50.98	82.04
1	220.16	286.73	310.21	332.13	351.04
2	361.0	400.69	413.97	421.68	426.18
3	427.46				
^{208}Pb					
0		0.24	8.50	20.18	34.61
1	168.19	276.30	287.30	300.27	313.89
2	330.45	372.19	389.29	402.62	412.34
3	403.72				

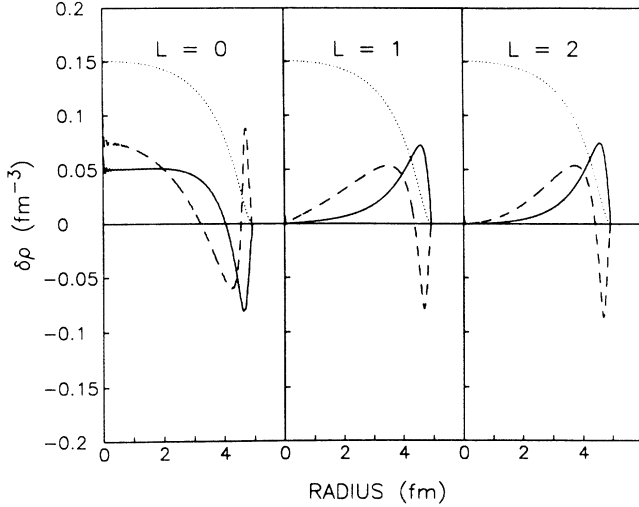


FIG. 1. Transition densities normalized by Eq. (26) of monopole ($L=0$), dipole ($L=1$), and quadrupole ($L=2$) eigenmodes of stability matrix $S(\mathbf{r},\mathbf{r}')$ for ^{40}Ca . The solid line is for the lowest level of each multipole mode and the dashed line is for the next level. The self-consistent density (dotted line) is also shown to indicate the surface of the nucleus.

$$\delta\rho_l(\mathbf{r}) \propto r^{l-1} \left[\frac{\partial}{\partial r} \rho(r) \right] Y_l^m(\hat{r}), \quad (42)$$

for $l > 0$.² Here, $l=0$ is excluded since the monopole vibration cannot be treated with the assumption of in-

compressibility. For $l=1$, Eq. (42) represents the translational motion of the whole nucleus. Using Eq. (20) and $\int d^3r' S(\mathbf{r},\mathbf{r}') \nabla' \rho(\mathbf{r}') = \nabla h(\mathbf{r})$ for $v(\mathbf{r},\mathbf{r}') = v(|\mathbf{r}-\mathbf{r}'|)$, we can show analytically that the translational mode is an eigensolution of the stability matrix with zero eigenvalue. We compared this transition density Eq. (42) of multipole vibration modes (dash-dotted line) to the zero node multipole mode of our stability matrix (solid line) in Fig. 2 for quadrupole ($l=2$) and octupole ($l=3$) modes. These transition densities are quite close to each other. For the transition density given by Eq. (42), we can get the expectation value of our stability matrix. These expectation values ϵ' are given in Table II together with the eigenvalues of stability matrix ϵ . These also are close to each other for small l . The nonzero values for $l=1$ represent numerical inaccuracy. The differences between the expectation values and the eigenvalues of stability matrix become larger for larger l and the eigenvalues are lower than the expectation values. The differences in the transition densities also become larger for larger l even though this may be hard to see in Fig. 2. This probably means the eigenmode of stability matrix is different from the multipole vibration mode in the simple nuclear fluid model at least for large l .

Now, let us consider the monopole mode which cannot be treated by Eq. (42). Due to its spherical symmetry, the simplest density variation for monopole mode we can consider is compression or expansion keeping the same form of density distribution of a nucleus. This can be

TABLE II. Stability and dispersion relation for the lowest multipole modes with $0 \leq l \leq 4$ (one node mode for $l=0$ and zero node for others). ϵ is the eigenvalue of the stability matrix Eq. (24), ϵ' is the expectation value of the stability matrix with the scaling density Eq. (43) for monopole or the transition density Eq. (42) for other multipoles, and $\langle \epsilon \rangle$ is the expectation value of the stability matrix with eigensolution of dispersion relation Eq. (56). These ϵ 's are in units of MeV fm^3 . $\langle \hbar\omega \rangle$ is the expectation value of vibration energy with the eigensolution of stability matrix Eq. (24) using Eq. (58), $\hbar\omega$ is the eigenvalue of dispersion relation Eq. (56), and $\hbar\omega'$ is the corresponding value using Eq. (58) and the eigensolution of dispersion relation. These $\hbar\omega$'s are in units of MeV . Nonzero values for dipole modes ($l=1$) indicate numerical error and i means pure imaginary, i.e., the corresponding ω^2 is negative.

l	ϵ	ϵ'	$\langle \epsilon \rangle$	$\langle \hbar\omega \rangle$	$\hbar\omega$	$\hbar\omega'$
For ^{16}O						
1	0.17	0.08	0.17	0.63	0.45	0.63
2	37.14	37.83	37.28	11.45	9.20	11.22
3	78.80	80.98	79.56	19.93	16.39	19.17
4	120.19	124.33	122.42	28.56	23.34	27.08
0	239.63	248.42	248.10	49.82	37.46	40.95
For ^{40}Ca						
1	-0.11	-0.20	-0.11	0.50 <i>i</i>	0.31 <i>i</i>	0.50 <i>i</i>
2	22.54	23.24	22.61	8.36	6.36	8.20
3	50.98	53.05	51.24	14.48	11.74	14.05
4	82.04	85.57	82.72	20.85	17.27	20.08
0	220.16	226.91	232.01	44.38	31.58	36.14
For ^{208}Pb						
1	0.24	0.15	0.24	0.77	0.35	0.77
2	8.50	8.99	8.54	4.80	2.93	4.74
3	20.18	21.84	20.33	7.96	5.59	7.79
4	34.61	37.53	34.89	11.28	8.55	10.97
0	168.19	170.78	189.79	32.62	20.39	27.58

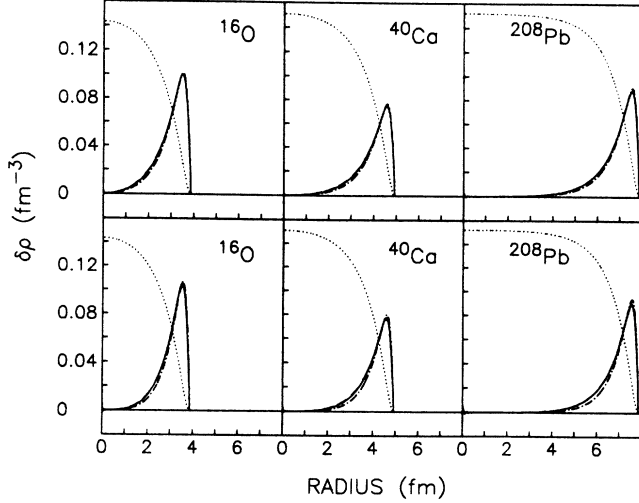


FIG. 2. Transition densities normalized by Eq. (26) for the lowest levels of quadrupole ($l=2$, upper row) and octupole ($l=3$, lower row) modes of ^{16}O , ^{40}Ca , and ^{208}Pb . The solid line is for the eigenmode of the stability matrix Eq. (24) and the dashed line, which is almost indistinguishable from the solid line, is for the eigenmode of the dispersion relation, Eq. (56). The dash-dotted line is for the irrotational and incompressible nucleus, i.e., Eq. (42). The curves for ^{208}Pb are twice the normalized transition densities. The self-consistent densities for each nucleus are also shown (dotted line).

represented by the scaling transformation of \mathbf{r} to $\alpha\mathbf{r}$ where $\alpha=1+\delta\alpha$ with infinitesimal $\delta\alpha$. Considering the nucleon number conservation, the new density due to this transformation becomes $\alpha^3\rho(\alpha\mathbf{r})$. The transition density² for this scaling is, for a spherical nucleus,

$$\delta\rho_s(\mathbf{r}) = \alpha^3\rho(\alpha\mathbf{r}) - \rho(\mathbf{r}) \approx \frac{1}{r^2} \frac{\partial}{\partial r} [r^3\rho(r)] \delta\alpha. \quad (43)$$

We can see this scaling density (dash-dotted line) is also similar to the eigensolution of stability matrix for lowest monopole mode (solid line) in Fig. 3. However, these have more differences than the zero node higher multipole case (Fig. 2). In Table II, we also compared the expectation values of stability matrix on the scaling density Eq. (43) to the lowest eigenvalues of the stability matrix Eq. (24). These are still comparable but the differences are larger than the zero node higher multipole case. The eigenvalues are smaller than the expectation values and the difference is larger for a smaller nucleus. This probably means the monopole mode of stability matrix has significant differences from the scaling mode.

In this section, we have shown that the stability condition for the self-consistent solution of the Vlasov equation is satisfied and that the eigenmodes of the stability matrix have very similar features to the multipole vibration modes. In the next section, we will consider time-dependent Vlasov solutions; assuming a periodic motion, we will try to relate the periodicity of vibration with the stability matrix.

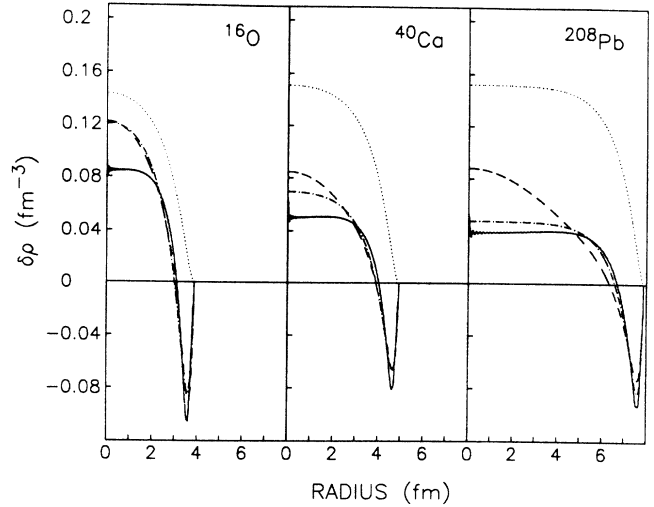


FIG. 3. Transition densities normalized by Eq. (26) for the lowest levels of monopole ($l=0$) modes of ^{16}O , ^{40}Ca , and ^{208}Pb . The solid line is for the eigenmode of the stability matrix Eq. (24) and the dashed line is for the eigenmode of the dispersion relation Eq. (56). The dash-dotted line is the normalized scaling density, Eq. (43). The curves for ^{208}Pb are twice the normalized transition densities. The self-consistent densities for each nucleus are also shown (dotted line).

IV. TIME-DEPENDENT VIBRATION MODE

In the preceding section, we have seen that there are close similarities between the eigensolutions of the stability matrix and the multipole vibration modes. To relate the eigenmodes of the stability matrix to the physical vibration modes of a nucleus, we should study the time-dependent behavior of the nucleus when the density is deviated initially from its equilibrium density. To consider a time-dependent vibration mode in a classical limit, we use the time-dependent Vlasov equation (3) with the time-dependent mean-field potential U given by Eq. (21) with time-dependent self-consistent density $\rho(\mathbf{r}, t)$. Since $\rho(\mathbf{r}, t) = \int d^3p f(\mathbf{r}, \mathbf{p}, t)$, integrating Eq. (3) over momentum gives us the continuity equation

$$\frac{\partial}{\partial t} \rho(\mathbf{r}, t) + \nabla \cdot \mathbf{J}(\mathbf{r}, t) = 0, \quad (44)$$

where the current density \mathbf{J} is

$$\mathbf{J}(\mathbf{r}, t) = \int d^3p \frac{\mathbf{p}}{m} f(\mathbf{r}, \mathbf{p}, t). \quad (45)$$

For the time-dependent problem, we need to consider nonzero current density which implies at least dipole deformation in the local Fermi sea, i.e., in the \mathbf{p} dependence of $f(\mathbf{r}, \mathbf{p}, t)$. This also implies that the Wigner function for a static nucleus should not linearly depend on the direction of \mathbf{p} . In the preceding two sections for a static nucleus, we have used the Wigner function of Eq. (8) which gives an isotropic Fermi surface at each point \mathbf{r} with Fermi momentum $\mathbf{p}_F(\mathbf{r})$.

Using Eq. (3), the time variation of the current density becomes

$$\begin{aligned} \frac{\partial}{\partial t} \mathbf{J}(\mathbf{r}, t) &= -\nabla \cdot \int d^3p \frac{\mathbf{p}}{m} \frac{\mathbf{p}}{m} f(\mathbf{r}, \mathbf{p}, t) \\ &+ [\nabla U(\mathbf{r}, t)] \cdot \int d^3p \frac{\mathbf{p}}{m} \nabla_p f(\mathbf{r}, \mathbf{p}, t) . \end{aligned}$$

The last term of this equation can be simplified using integration by parts with dropping the surface integral and using $[\nabla U(\mathbf{r})] \cdot \nabla_p \mathbf{p} = \nabla U(\mathbf{r})$. Separating the rank 0 part and rank 2 part, the kinetic pressure tensor $\vec{\mathbf{P}}$ becomes

$$\vec{\mathbf{P}}(\mathbf{r}, t) = \frac{1}{m} \int d^3p \mathbf{p} \mathbf{p} f(\mathbf{r}, \mathbf{p}, t) = \frac{2}{3} T(\mathbf{r}, t) \vec{\mathbf{I}} + \frac{1}{3} \frac{1}{m} \vec{\mathbf{Q}}(\mathbf{r}, t) ,$$

where $\vec{\mathbf{I}}$ is unit tensor. The kinetic energy density $T(\mathbf{r}, t)$ and the traceless quadrupole moment tensor $\vec{\mathbf{Q}}(\mathbf{r}, t)$ of the local Fermi sea are

$$T(\mathbf{r}, t) = \frac{1}{2} \sum_k P_{kk}(\mathbf{r}, t) = \int d^3p \frac{p^2}{2m} f(\mathbf{r}, \mathbf{p}, t) , \quad (46)$$

$$\begin{aligned} Q_{ij}(\mathbf{r}, t) &= \hat{\mathbf{i}} \cdot [\hat{\mathbf{j}} \cdot \vec{\mathbf{Q}}(\mathbf{r}, t)] \\ &= m \left[3P_{ij}(\mathbf{r}, t) - \sum_k P_{kk}(\mathbf{r}, t) \delta_{ij} \right] \\ &= \int d^3p p^2 [3(\hat{\mathbf{i}} \cdot \hat{\mathbf{p}})(\hat{\mathbf{j}} \cdot \hat{\mathbf{p}}) - (\hat{\mathbf{i}} \cdot \hat{\mathbf{j}})] f(\mathbf{r}, \mathbf{p}, t) . \end{aligned} \quad (47)$$

Here $\hat{\mathbf{p}}$ is the unit vector of \mathbf{p} and $\hat{\mathbf{i}}$ and $\hat{\mathbf{j}}$ are the unit vectors of the orthogonal coordinate system. Notice that $T(\mathbf{r}, t)$ here is not of the form of Eq. (10) since we are considering a general Wigner function for which the local Fermi momentum should depend on $\hat{\mathbf{p}}$ at least linearly. The quadrupole moment tensor is related to the kinetic pressure tensor through Eq. (47). Finally, we have the time variation of the current density as

$$\begin{aligned} \frac{\partial}{\partial t} \mathbf{J}(\mathbf{r}, t) &= -\frac{2}{3} \frac{1}{m} \nabla T(\mathbf{r}, t) - \frac{1}{m} \rho(\mathbf{r}, t) \nabla U(\mathbf{r}, t) \\ &- \frac{1}{3} \frac{1}{m^2} \nabla \cdot \vec{\mathbf{Q}}(\mathbf{r}, t) . \end{aligned} \quad (48)$$

$$\begin{aligned} \rho(\mathbf{r}, t) &= \rho(\mathbf{r}) + \delta\rho(\mathbf{r}, t) \\ &= \frac{4\pi}{3} \frac{4}{h^3} p_F^3(\mathbf{r}) + p_F^2(\mathbf{r}) \int d\Omega_p \delta F(\mathbf{r}, \hat{\mathbf{p}}, t) + O((\delta F)^2) , \end{aligned}$$

$$\begin{aligned} T(\mathbf{r}, t) &= T(\mathbf{r}) + \delta T(\mathbf{r}, t) \\ &= \frac{4\pi}{5} \frac{4}{h^3} \frac{1}{2m} p_F^5(\mathbf{r}) + \frac{1}{2m} p_F^4(\mathbf{r}) \int d\Omega_p \delta F(\mathbf{r}, \hat{\mathbf{p}}, t) + O((\delta F)^2) \\ &= C\rho^{5/3}(\mathbf{r}, t) + O((\delta F)^2) , \end{aligned}$$

$$J_i(\mathbf{r}, t) = \hat{\mathbf{i}} \cdot \mathbf{J}(\mathbf{r}, t) = \frac{1}{m} p_F^3(\mathbf{r}) \int d\Omega_p (\hat{\mathbf{i}} \cdot \hat{\mathbf{p}}) \delta F(\mathbf{r}, \hat{\mathbf{p}}, t) + O((\delta F)^2) ,$$

$$Q_{ij}(\mathbf{r}, t) = p_F^4(\mathbf{r}) \int d\Omega_p [3(\hat{\mathbf{i}} \cdot \hat{\mathbf{p}})(\hat{\mathbf{j}} \cdot \hat{\mathbf{p}}) - (\hat{\mathbf{i}} \cdot \hat{\mathbf{j}})] \delta F(\mathbf{r}, \hat{\mathbf{p}}, t) + O((\delta F)^2) .$$

In writing $T(\mathbf{r}, t) = C\rho^{5/3}(\mathbf{r}, t) + O((\delta F)^2)$, we have used the equations immediately above it. Notice the kinetic energy density $T(\mathbf{r}, t)$ is the same as Eq. (10) up to first order in δF . Thus we should consider only up to first order in δF when we compare the discussions in this section to the stability equation of preceding sections.

Since $\frac{2}{3} \nabla \rho^{5/3} = \rho \nabla [(\partial \rho^{5/3}) / (\partial \rho)]$, Eq. (49) becomes

Combining Eqs. (44) and (48), we get the second-order time variation of the density as

$$\begin{aligned} \frac{\partial^2}{\partial t^2} \rho(\mathbf{r}, t) &= \frac{2}{3} \frac{1}{m} (\nabla \cdot \nabla) T(\mathbf{r}, t) + \frac{1}{m} \nabla \cdot [\rho(\mathbf{r}, t) \nabla U(\mathbf{r}, t)] \\ &+ \frac{1}{3} \frac{1}{m^2} \nabla \cdot [\nabla \cdot \vec{\mathbf{Q}}(\mathbf{r}, t)] . \end{aligned} \quad (49)$$

If there is no quadrupole deformation in the local Fermi sea, i.e., $\vec{\mathbf{Q}} = 0$, the last term in Eq. (49) is zero.

To study the vibration mode with a theta function type of Wigner function which represents the Hartree-Fock density matrix condition $\rho^2 = \rho$ in a classical approximation, we should allow the \mathbf{p} dependence in the local Fermi momentum p_F . For the single valued Fermi surface in any direction $\hat{\mathbf{p}}$ at a point \mathbf{r} , the most general Wigner function can be described by $f(\mathbf{r}, \mathbf{p}, t) = (4/h^3) \theta(p_F(\mathbf{r}, \hat{\mathbf{p}}, t) - p)$. Considering small amplitude vibrations from a static nucleus, the local Fermi momentum can be described by $p_F(\mathbf{r}, \hat{\mathbf{p}}, t) = p_F(\mathbf{r}) + \delta p_F(\mathbf{r}, \hat{\mathbf{p}}, t)$ where $p_F(\mathbf{r})$ may be taken to be the unperturbed static value of the Fermi surface at the point \mathbf{r} and $\delta p_F(\mathbf{r}, \hat{\mathbf{p}}, t) = (h^3/4) \delta F(\mathbf{r}, \hat{\mathbf{p}}, t)$ will be the small deviation. Thus the Wigner function can be written as

$$\begin{aligned} f(\mathbf{r}, \mathbf{p}, t) &= \frac{4}{h^3} \theta(p_F(\mathbf{r}) - p + (h^3/4) \delta F(\mathbf{r}, \hat{\mathbf{p}}, t)) \\ &= f_0(\mathbf{r}, \mathbf{p}) + \delta f(\mathbf{r}, \mathbf{p}, t) , \\ \delta f(\mathbf{r}, \mathbf{p}, t) &= \delta(p_F(\mathbf{r}) - p) \delta F(\mathbf{r}, \hat{\mathbf{p}}, t) + O((\delta F)^2) , \end{aligned} \quad (50)$$

where $f_0(\mathbf{r}, \mathbf{p})$ is the unperturbed part and given by Eq. (8) in the Thomas-Fermi approximation. For this Wigner function,

$$\begin{aligned} \frac{\partial^2}{\partial t^2} \rho(\mathbf{r}, t) &= \frac{1}{m} \nabla \cdot [\rho(\mathbf{r}, t) \nabla h(\mathbf{r}, t)] \\ &+ \frac{1}{3} \frac{1}{m^2} \nabla \cdot [\nabla \cdot \vec{\mathbf{Q}}(\mathbf{r}, t)] , \end{aligned} \quad (52)$$

where the time-dependent mean-field Hamiltonian $h(\mathbf{r}, t)$ is

$$h(\mathbf{r}, t) = \frac{\delta T(\mathbf{r}, t)}{\delta \rho(\mathbf{r}, t)} + U(\mathbf{r}, t) \\ = \frac{5}{3} C \rho^{2/3}(\mathbf{r}, t) + U(\mathbf{r}, t) + O((\delta F)^2). \quad (53)$$

This is exactly the same form as Eq. (16) up to first order in δF with the time-dependent density $\rho(\mathbf{r}, t)$. The time-independent part of $h(\mathbf{r}, t)$ is the same as Eq. (16) which is λ inside the nucleus due to the self-consistent equation (20) for the static density $\rho(\mathbf{r})$. Thus the zeroth order in δF of Eq. (52) is automatically satisfied and the first order terms give us a relation for $\delta\rho$ as

$$\frac{\partial^2}{\partial t^2} \delta\rho(\mathbf{r}, t) = \frac{1}{m} \nabla \cdot \left[\rho(\mathbf{r}) \nabla \left[\int d^3 r' S(\mathbf{r}, \mathbf{r}') \delta\rho(\mathbf{r}', t) \right] \right] \\ + \frac{1}{3} \frac{1}{m^2} \nabla \cdot [\nabla \cdot \vec{Q}(\mathbf{r}, t)], \quad (54)$$

where

$$S(\mathbf{r}, \mathbf{r}') = \left. \frac{\delta h(\mathbf{r}, t)}{\delta \rho(\mathbf{r}', t)} \right|_{\rho(\mathbf{r}, t) = \rho(\mathbf{r})} \\ = \left[\frac{10}{9} C \rho^{-1/3}(\mathbf{r}) + \sum_i C_i \sigma_i \rho^{\sigma_i - 1}(\mathbf{r}) \right] \\ \times \delta(\mathbf{r} - \mathbf{r}') + v(\mathbf{r}, \mathbf{r}') \quad (55)$$

and is the same as the stability matrix Eq. (17) in Sec. II. Here, we consider only the inside of the nucleus since $\delta\rho$ and \vec{Q} are zero up to first order in δF when $\rho=0$ due to the p_F dependence in Eq. (51). Notice here that both $\delta\rho(\mathbf{r}, t)$ and $\vec{Q}(\mathbf{r}, t)$ are unknown in Eq. (54). Thus this equation is not an eigenvalue equation for $\delta\rho$. Since it gives the relation between the frequency ω and the wave vector \mathbf{k} of the transition density $\delta\rho(\mathbf{r}, t)$ for a given $\vec{Q}(\mathbf{r}, t)$, we call Eq. (54) a dispersion relation of the transition density of a nucleus in the time-dependent Vlasov equation. The same stability matrix Eq. (17) appears in this dispersion relation for the vibration mode. Thus, this dispersion relation allows us to give physical interpretations to the eigenmodes of the stability matrix, connecting them with the vibrational modes of the nucleus. We should notice here that Eqs. (24) and (54) are consistent, i.e., the stability matrix S in Eq. (24) is the same as in Eq. (54), only up to first-order approximation in δF since $T(\mathbf{r}, t)$ in Eq. (51) is equivalent to $T(\mathbf{r})$ given by Eq. (10) only up to first order in δF . If we know the exact expression of $T(\mathbf{r}, t)$ in terms of $\rho(\mathbf{r}, t)$, then Eqs. (24) and (54) become exact by using the first expressions of Eqs. (53) and (55).

For an eigenmode of the stability matrix $S(\mathbf{r}, \mathbf{r}')$ [Eq. (17) or (55)], the spatial dependence of $\delta\rho$ should satisfy Eq. (24). Since the integral part in the parentheses of the first term in Eq. (54) is the same as the left-hand side of Eq. (24), the dispersion relation Eq. (54) gives the relation between the eigenvalue ϵ of the stability equation and the corresponding frequency ω of the time dependence of

$\delta\rho(\mathbf{r}, t)$ when we consider small vibrations of a nucleus from its equilibrium density. Since $\vec{Q}(\mathbf{r}, t)$ is also unknown, Eq. (54) does not determine the frequency ω directly for a given transition density $\delta\rho(\mathbf{r}, t)$. However, in Sec. II for the stability condition, we have considered a Fermi sphere which is spherically symmetric and has no quadrupole deformation. Thus, to relate the stability condition with vibration modes, we can neglect the \vec{Q} dependent term in the dispersion relation Eq. (54) which becomes an eigenvalue equation (wave equation) for $\delta\rho$ as

$$\frac{\partial^2}{\partial t^2} \delta\rho(\mathbf{r}, t) = -\omega^2 \delta\rho(\mathbf{r}, t) \\ = \frac{1}{m} \nabla \cdot \left[\rho(\mathbf{r}) \nabla \left[\int d^3 r' S(\mathbf{r}, \mathbf{r}') \delta\rho(\mathbf{r}', t) \right] \right]. \quad (56)$$

This equation determines the spatial dependence of the transition density for an eigenmode of vibration with eigenvalue ω^2 . Notice here that the term multiplied by $\delta\rho(\mathbf{r}', t)$ in the right-hand side of this eigenvalue equation is not symmetric in \mathbf{r} and \mathbf{r}' in contrast with the stability matrix $S(\mathbf{r}, \mathbf{r}')$. Once we know the spatial dependence of a transition density $\delta\rho(\mathbf{r})$, we can find the expectation value of ω^2 [Eq. (56)] for this $\delta\rho$ by

$$\omega^2 = \frac{1}{m} \int d^3 r \rho(\mathbf{r}) [\nabla g(\mathbf{r})] \\ \cdot \left[\nabla \left[\int d^3 r' S(\mathbf{r}, \mathbf{r}') g(\mathbf{r}') \right] \right], \quad (57)$$

where $g(\mathbf{r})$ is the normalized spatial dependence of $\delta\rho(\mathbf{r}, t)$. Using Eq. (24) for an eigenmode of the stability matrix, we get

$$\omega^2 = \frac{\epsilon}{m} \int d^3 r \rho(\mathbf{r}) [\nabla g(\mathbf{r})] \cdot [\nabla g(\mathbf{r})]. \quad (58)$$

This relation connects the eigenvalue ϵ of the stability matrix to the frequency ω . Equation (58) shows that the stability condition, which requires positive eigenvalues ϵ of the stability matrix, is related to the requirement that the frequencies ω are all real for the time-dependent vibration of the density.

On the other hand, let us consider the eigensolutions of Eq. (56). Since the right-hand side of Eq. (56) is not symmetric in \mathbf{r} and \mathbf{r}' , eigenvectors $\delta\rho$ of this equation are not orthogonal to each other. However, $S(\mathbf{r}, \mathbf{r}')$ has all positive real eigenvalues except for one zero eigenvalue as we have seen in Sec. III, hence we can show that the orthogonality condition becomes

$$\int d^3 r d^3 r' g_i(\mathbf{r}) S(\mathbf{r}, \mathbf{r}') g_j(\mathbf{r}') \propto \delta_{ij}, \quad (59)$$

where $g(\mathbf{r})$ is the normalized spatial dependence of the eigensolution $\delta\rho(\mathbf{r}, t)$ of Eq. (56). This orthogonality condition Eq. (59) is exactly the same as Eq. (23), the stability condition. Using this orthogonality condition, we get, from Eq. (56),

$$\omega^2 \int d^3 r_1 d^3 r g(\mathbf{r}_1) S(\mathbf{r}_1, \mathbf{r}) g(\mathbf{r}) = \frac{1}{m} \int d^3 r \rho(\mathbf{r}) \left[\nabla \left[\int d^3 r_1 g(\mathbf{r}_1) S(\mathbf{r}_1, \mathbf{r}) \right] \right] \cdot \left[\nabla \left[\int d^3 r' S(\mathbf{r}, \mathbf{r}') g(\mathbf{r}') \right] \right]. \quad (60)$$

Since the right-hand side of Eq. (60) is positive definite, the positive eigenvalue ω^2 of Eq. (56) means the stability of our static Vlasov solution. This statement is just the same as in the Hartree-Fock case. In Hartree-Fock, the stability condition of the static solution requires that the eigenvalues of the RPA matrix of TDHF be all real.

Numerical solution of Eq. (56) shows that all the eigenvalues ω^2 are real and positive except for the lowest level of the dipole mode which corresponds to the translational mode of the whole nucleus with zero eigenvalue. Since translation is an eigenmode of the stability matrix with zero eigenvalue as we discussed in the preceding section, the right-hand side of Eq. (56) becomes zero. Furthermore, the translation of the whole nucleus induces only monopole and dipole deformations of the local Fermi sea and thus $\bar{Q}=0$. Thus the translational mode is a common eigensolution of both the stability matrix and the dispersion relation Eq. (54) with zero eigenvalue. The transition densities of the lowest modes of Eq. (56) for $l > 1$, which have no node, are strikingly similar to the lowest eigenmodes of the stability matrix. These are indistinguishable in Fig. 2 (dashed line and solid line) except that there are small ripples inside of the nucleus for the stability matrix case. These are approximately the same as the transition density given by Eq. (42) (dash-dotted line in Fig. 2) which is obtained from the irrotational and incompressible flow approximations. The expectation values of the stability matrix for these zero node modes of Eq. (56) ($\langle \epsilon \rangle$ in Table II) are the same as the eigenvalues of the stability matrix with zero node (ϵ in Table II) within numerical error. The transition densities of higher eigenmodes which have at least one node are, of course, different since those of the dispersion relation are not orthogonal to each other while those of the stability matrix are orthogonal to each other.

For the lowest eigenmode of the monopole case which has one node, the departures from the scaling density Eq. (43) (dash-dotted line in Fig. 3) are opposite between the dispersion relation Eq. (56) (dashed line) and the stability matrix Eq. (24) (solid line). For a small nucleus, the scal-

ing density is a good approximation to the eigensolution of the dispersion relation (they are almost the same for ^{16}O in Fig. 3). For a large nucleus, the scaling density is rather similar to the eigensolution of the stability matrix (^{208}Pb in Fig. 3). For an intermediate mass nucleus, the scaling density is between the eigensolutions of the stability matrix and the dispersion relation (^{40}Ca in Fig. 3). We also show the transition densities of two node monopole modes in Fig. 4. The eigensolution of the dispersion relation is more centrally peaked than the eigensolution of the stability matrix for monopole modes (Figs. 3 and 4). We have seen the same behavior in the eigenmodes of higher multipoles ($l > 0$) with at least one node.

We show the vibration energy $\langle \hbar\omega \rangle$ calculated by Eq. (58) for the transition density of the lowest eigenmode of the stability matrix and $\hbar\omega$ of the lowest eigenvalue of Eq. (56) in Table II. In this table, $\hbar\omega'$ is calculated by Eq. (58) for the eigenmodes of Eq. (56). Table II shows that the general dependence on l and nuclear sizes of the vibration energy corresponding to the eigenmodes of the stability matrix Eq. (24) and the dispersion relation Eq. (56) are similar to those seen in the actual resonance energy of multipole vibration modes.

The departures of lowest eigenmode of Eq. (56) (dashed line) for monopole (Fig. 3) and quadrupole mode (Fig. 2) from the transition densities in Eqs. (43) and (42), respectively (dash-dotted line), are similar to those seen in Ref. 18 for ^{208}Pb using RPA with SkI interaction. Our eigenvalue ω for ^{208}Pb (Table II) is similar to the RPA result ($\hbar\omega=20$ MeV) for monopole mode but much smaller than the RPA result ($\hbar\omega=11.4$ MeV) for quadrupole mode. The small value of $\hbar\omega$ compared to the giant resonance energy (for example, $\hbar\omega=3$ MeV for quadrupole mode of ^{208}Pb compared to about 10 MeV of empirical value) indicates that we cannot neglect the contribution from the $\bar{Q}(\mathbf{r}, t)$ term of Eq. (54) to study eigenmodes of giant resonances. It is well known that, without quadrupole deformation of Fermi sea (liquid drop model), the vibration energy is much lower than the giant multipole modes.^{2,13,19} Our eigenvalues $\hbar\omega$ of Eq. (56) are quite similar to the surface vibration modes of the liquid drop model which are close to the low-lying multipole modes rather than to giant resonances. The effects of the quadrupole-dependent term are discussed in Ref. 20.

V. CONCLUSION

The stability condition of a self-consistent Thomas-Fermi solution can be cast in the form of matrix equation; for stability, the eigenvalues of the stability matrix must be all positive. The same stability matrix also appears in the dispersion relation derived from the time-dependent Vlasov equation for small amplitude oscillations. This makes it possible to relate the stability matrix to the normal modes of the nucleus. For excitations which do not involve quadrupole deformation of the Fermi sea, the stability condition requiring all the eigenvalues of the stability matrix to be real positive is exactly equivalent to requiring the corresponding oscillation frequency ω to be real. This feature makes the analogy with quantum calculations quite striking; the stability of static Hartree-Fock solution is guaranteed if the eigenvalues

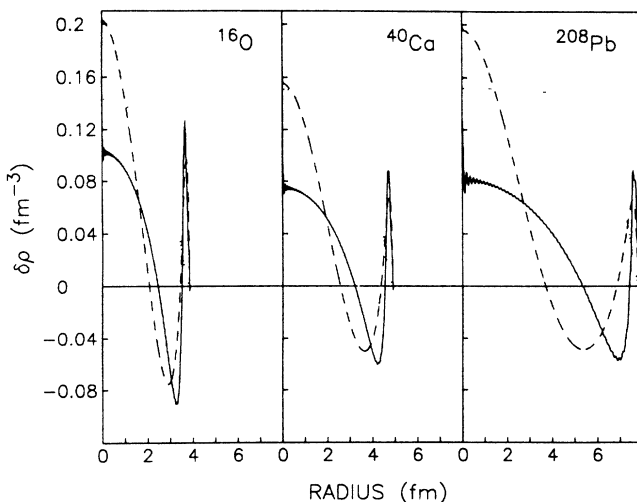


FIG. 4. Same as in Fig. 3 but for the next levels of monopole ($l=0$) modes.

(oscillation frequencies) of the RPA matrix are all real.

In the quantum case, experience in nuclear physics shows that the eigenfunctions of the RPA matrix correspond to collective excitations in the nucleus; in a similar fashion, the lowest eigenfunctions of the stability matrix correspond to easily recognizable multipole modes in the nucleus. The oscillation frequencies evaluated with dispersion relation for these modes are similar to the values of the surface oscillations in a liquid drop model which correspond to the low-lying multipole modes. If

we know the quadrupole moment of the Fermi sea for each multipole vibration, the dispersion relation can be applied to study giant resonances.

ACKNOWLEDGMENTS

Discussions with N. de Takacsy are gratefully acknowledged. This work was supported in part by the Natural Sciences and Engineering Research Council of Canada and in part by the Québec Department of Education.

¹G. F. Bertsch and S. Das Gupta, *Phys. Rep.* **160**, 189 (1988).

²P. Ring and P. Schuck, *The Nuclear Many-Body Problem* (Springer-Verlag, New York, 1980).

³H. H. K. Tang, C. H. Dasso, H. Esbensen, R. A. Broglia, and A. Winther, *Phys. Lett.* **101B**, 10 (1981).

⁴H. H. Gan, S. J. Lee, and S. Das Gupta, *Phys. Rev. C* **36**, 2365 (1987).

⁵S. J. Lee, H. H. Gan, E. D. Cooper, and S. Das Gupta, *Phys. Rev. C* **40**, 2585 (1989).

⁶R. J. Lenk and V. R. Pandharipande, University of Illinois report, 1989.

⁷P. J. Siemens, *Phys. Rev. C* **1**, 98 (1970).

⁸S. J. Lee and S. Das Gupta (unpublished).

⁹D. J. Thouless, *Nucl. Phys.* **21**, 225 (1960).

¹⁰D. J. Thouless, *Nucl. Phys.* **22**, 78 (1961).

¹¹L. H. Thomas, *Proc. Cambridge Philos. Soc.* **23**, 542 (1927).

¹²E. Fermi, *Z. Phys.* **48**, 73 (1928).

¹³G. F. Bertsch, in *Nuclear Physics with Heavy Ions and Mesons*, Les Houches Session XXX, 1977, edited by R. Balian, M. Rho, and G. Ripka (North-Holland, Amsterdam, 1978), Vol. 1, p. 175.

¹⁴D. Brink, A. Dellafiore, and M. Di Toro, *Nucl. Phys.* **A456**, 205 (1986).

¹⁵G. F. Burgio and M. Di Toro, *Nucl. Phys.* **A476**, 189 (1988).

¹⁶P. Bonche, S. Koonin, and J. W. Negele, *Phys. Rev. C* **13**, 1226 (1976).

¹⁷E. Suraud, M. Barranco, and J. Treiner, *Nucl. Phys.* **A480**, 29 (1988).

¹⁸G. F. Bertsch and S. F. Tsai, *Phys. Rep.* **18C**, 125 (1975).

¹⁹A. Bohr and B. R. Mottelson, *Nuclear Structure* (Benjamin, New York, 1969), Vol. II.

²⁰S. J. Lee, H. H. Gan, E. D. Cooper, and S. Das Gupta (unpublished).